YALE PEABODY MUSEUM

JOURNAL OF MARINE RESEARCH

The *Journal of Marine Research,* one of the oldest journals in American marine science, published important peer-reviewed original research on a broad array of topics in physical, biological, and chemical oceanography vital to the academic oceanographic community in the long and rich tradition of the Sears Foundation for Marine Research at Yale University.

An archive of all issues from 1937 to 2021 (Volume 1–79) are available through EliScholar, a digital platform for scholarly publishing provided by Yale University Library at https://elischolar.library.yale.edu/.

Requests for permission to clear rights for use of this content should be directed to the authors, their estates, or other representatives. The *Journal of Marine Research* has no contact information beyond the affiliations listed in the published articles. We ask that you provide attribution to the *Journal of Marine Research.*

Yale University provides access to these materials for educational and research purposes only. Copyright or other proprietary rights to content contained in this document may be held by individuals or entities other than, or in addition to, Yale University. You are solely responsible for determining the ownership of the copyright, and for obtaining permission for your intended use. Yale University makes no warranty that your distribution, reproduction, or other use of these materials will not infringe the rights of third parties.

Describing additional fluxes to deep sediment traps and water-column decay in a coastal environment

by David A. Timothy[1] and Stephen Pond[1]

ABSTRACT

Sediment traps were moored at three stations in Sechelt Inlet, a fjord in southern British Columbia, Canada, for five one-month deployment periods from late January to late June, 1991. On each mooring were traps at three depths; total and constituent fluxes often increased with depth. We present the flux data and describe an analytical model that is based on a set of simultaneous equations for which two unknowns are the decay rate of material representatively caught by two vertically-separated sediment traps and the composition of material causing observed increases in flux with depth. The unknowns are solved in a least-squares sense and the results indicate that 60–71% of organic carbon, 57–62% of nitrogen and 41–48% of biogenic silica were lost from the particulate phase over a 200 m depth interval during the study. The results also suggest that material contributing additional fluxes to deep traps was compositionally similar to material settling from traps above.

1. Introduction

In studies of vertical particle flux in the ocean using moored sediment traps, increases in flux with depth are often observed, especially in coastal environments. For these situations, deducing particulate supply from surface waters as well as the alteration of material as it sinks is not straightforward without a means of separating primary fluxes from the additional material caught by deep traps.

Quantitative methods to interpret sediment-trap fluxes that increase with depth have considered either the decay of primary fluxes or the composition and amount of additional fluxes, but not both simultaneously. For instance, a technique to investigate water-column decay involves the normalization of reactive components to a conservative element. Noriki and Tsunogai (1986), for trap fluxes from the Pacific and Southern Oceans, and Walsh *et al.* (1988a), for the Equatorial North Pacific, both normalized fluxes of particulate organic carbon, calcium carbonate and biogenic silica to aluminum (Al). Their estimates of remineralization give similar amounts of biogenous flux decay over comparable depth intervals. However, the normalization procedure assumes compositional similarity between primary and additional fluxes, a constraint that is not everywhere appropriate. For example, artificially high decay rates are obtained if Al-rich material, such as refractory

bottom sediment, is the cause of an increase in flux with depth (Walsh *et al.,* 1988a). Normalization to Al also assumes that the Al flux is conservative, though dissolved Al is known to be scavenged by sinking particles (Orians and Bruland, 1986). In regions where Al fluxes are small, scavenging may cause overestimates of decay. Bloesch (1982) applied a method to quantify the amount of resuspended material that reached near-bottom traps in the shallow and turbulent waters of Lake Erie. The method was able to detect that there were both locally resuspended sediments and material of a more organic-rich nature within the additional flux to hypolimnetic traps. Walsh and Gardner (1992) described a similar model and found that the composition of the additional flux to deeper traps moored in the Gulf of Mexico was more similar to the primary flux than to bottom sediments. However, these two techniques were not general because water-column decay was either not considered (Bloesch, 1982) or had to be estimated independently using the normalization scheme (Walsh and Gardner, 1992).

Three common methods to unravel coastal sediment-trap fluxes that increase with depth were reviewed by Håkanson *et al.* (1989), and a combination of two of those methods (the base-line approach and the burial approach) was used by Pejrup *et al.* (1996) to separate primary from resuspended fluxes in a shallow, coastal environment. Techniques similar to the label approach of Håkanson *et al.* (1989) have been used to infer much about processes affecting particles as they sink. For instance, a greater abundance and different assemblages of intact phytoplankton cells in deep sediment traps relative to shallow traps was used to evaluate the degree of lateral transport from the shelf to the slope of the Middle Atlantic Bight (Falkowski *et al.,* 1994). The composition of sediment-trap material and underlying sediments has provided insight into the biochemical changes that occur to particles as they sink through the water column and become incorporated into the sediments in Dabob Bay, WA (Hedges *et al.,* 1988a,b). However, none of the approaches outlined by Håkanson *et al.* (1989) describe remineralization of the primary flux, a term that may be relatively large where water depths are greater than roughly 10 to 100 m (Pejrup *et al.,* 1996).

The primary concern of our work is to estimate water-column decay rates of settling particulate material where observed fluxes increase with depth so that elemental budgets can be described for these regions. We have formulated a general balance equation model that treats as unknowns both water-column decay and the composition of additional material caught by a deeper trap. We apply the model to fluxes of particulate organic carbon, particulate nitrogen, biogenic silica and lithogenous matter during a five-month study in Sechelt Inlet, British Columbia.

2. Materials and methods

a. Experiment location and design

Sechelt Inlet is a system of fjords (Sechelt, Salmon and Narrows Inlets) on the mainland side of the Strait of Georgia in southern British Columbia, Canada (Fig. 1). The primary freshwater input to the system is through the Clowhom River at the head of Salmon Inlet.
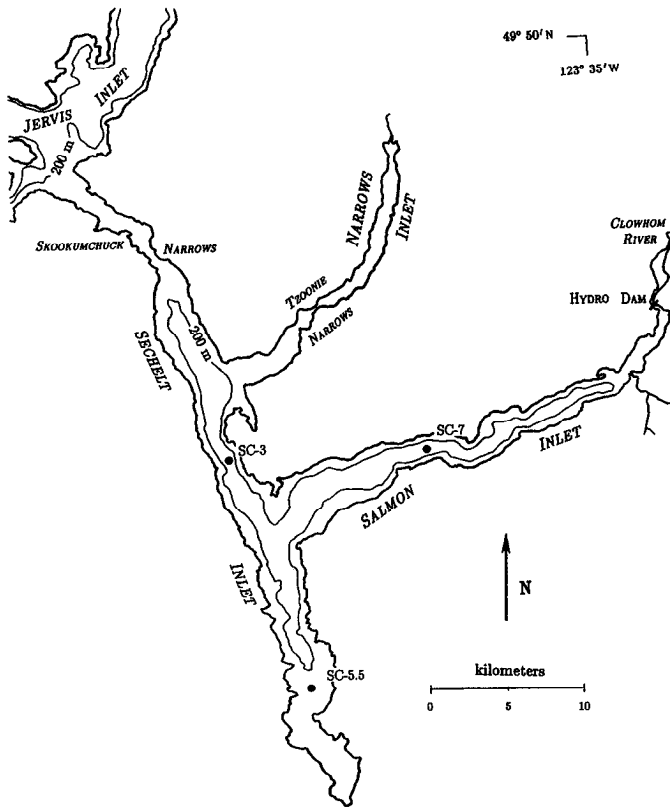
Figure 1. Sechelt Inlet and sediment-trap mooring sites.

Since no sill separates Salmon Inlet from the body of Sechelt Inlet, the main axis of the system is considered to be along the path of principal estuarine flow, from the head of Salmon Inlet to the mouth of Sechelt. Two shallow sills within the system are at Skookumchuck Narrows (14 m sill) and at Tzoonie Narrows (11 m sill). The constricted passage at Skookumchuck Narrows causes turbulent tidal jets to reach speeds up to 8 m s^{-1} (one of the stronger currents in British Columbia coastal waters), but these currents quickly dissipate as the inlet widens and deepens. The drainage basin of the system is small relative to other inlets in British Columbia; annually-averaged terrestrial run-off is about 110 m^3 s^{-1} (Pickard, 1961). Sechelt Inlet is not known to develop anoxia, although dissolved oxygen concentrations were as low as 10–30 mmoles m^{-3} in the deep waters during the study. Deep water renewal occurs in the late winter to early spring, but not every year. A deep water renewal was not detected during this experiment, but there was some replacement to mid-depth between February and March (Tinis, 1995).

Sediment traps were moored at stations SC-3, SC-5.5, and SC-7 (Fig. 1). Total water depth at the three stations is 280 m, 180 m and 265 m, respectively. Moorings were first deployed on January 23, and serviced on February 19, March 26–27, April 23–24, May

22–23 and June 22–23, 1991. Thus, there were five deployment periods, which will be referred to by the month for which they were most operative: the first sampling period will be referred to as the February deployment, and so on. For each mooring, traps were positioned 50 m from the surface, 50 m from the bottom and at mid-depth. This arrangement was chosen so that the upper traps would be below the base of the euphotic zone (the average 1% light level during the experiment was 17 m; Timothy, 1994) and the lower traps would be away from the sediment-water interface.

The sediment traps, designed by K. Iseki, F. Whitney and C. S. Wong (unpubl.), were made from PVC cylinders with an inside diameter of 12.7 cm, a wall thickness of 0.70 cm and a height of 48 cm, giving an aspect ratio (I.D./height) of 3.8. Flat bottomed, cylindrical collection chambers that fit snuggly into the base of each trap allowed separation of collected sediment from traps after retrieval. The collection chambers were 6.4 cm tall with inside diameter of 11.4 cm and outside diameter of 12.6 cm. Baffle grids (1.5 cm square) were placed in the opening (baffle height of 5.1 cm) and in the collection chamber (baffle height of 6.4 cm) of each trap. The purpose of the baffles was to decrease the effects of turbulent mixing within the traps throughout the sampling period and during recovery (Gardner, 1980). Prior to deployment, traps were filled with seawater. 500 ml of 30% NaCl solution were then funneled to the bottom of the traps, displacing the volume of the sample chambers to a depth of about 0.5 diameter equivalents and giving the traps an aspect ratio of 3.3 above the brine layer. The brine solution was meant to reduce *in situ* bacterial activity and to create a density gradient with ambient seawater so that turbulent mixing and loss of intercepted material would be minimized. Sediment traps were always deployed in pairs. In one trap of each pair, the NaCl solution also contained 0.5% sodium azide (NaN_3) as a bactericide. NaN_3 inhibits aerobic but not anaerobic bacterial respiration and acts as a poison to zooplankton that may be attracted to material caught by traps.

The sediment-trap experiment was part of a larger effort to study the biology and physics of Sechelt Inlet. Water samples were collected from five depth intervals (0–1.5, 1.5–3, 3–6, 9–12, 18–21 m) at five stations throughout the inlet using a segmented-pipe sampler (Sutherland *et al.,* 1992) for the measurement of chlorophyll *a* and phaeopigments by the fluorometric method of Parsons *et al.* (1984). Aloquots from the water samples were preserved with acidic Lugol's solution for later phytoplankton identification and enumeration by the Utermöhl technique (Hasle, 1978). Current meters (InterOcean S4, Aanderaa and cyclesondc; Tinis, 1995) were moored at three stations for the duration of the sediment-trap experiment. One of the current meter arrays was close to the sediment-trap mooring at station SC-3.

b. Sample treatment and analyses

Upon retrieval, the sediment-trap samples were filtered through 0.47 mm Nitex monofilament bolting cloth to remove large zooplankton and other swimmers. In the laboratory, the samples were washed free of salt by repetitive centrifugation with deionized water. The solid phase was freeze-dried, weighed and ground to a fine powder. Total carbon and

nitrogen were determined by gas-chromatography on a model 1106 Carlo-Erba CHN analyzer calibrated with acetanilide ($CH_3CONC_6H_5$) with an analytical precision (1σ) of $\pm 1.3\%$ for carbon and $\pm 2\%$ for nitrogen. Inorganic carbon was measured on a Coulometrics Inc. CO_2 coulometer ($\sigma = \pm 2\%$) and converted to $CaCO_3$. Particulate organic carbon (POC) was determined by subtracting inorganic carbon from total carbon. Biogenic silica was measured following the method and equations of Mortlock and Froelich (1989). The procedure involves extracting amorphous silica from a sediment sample with 2 M Na_2CO_3 and then measuring the dissolved silicon concentration in the extract by molybdate-blue spectrophotometry. Conversion from biogenic silicon (%Si) to biogenic silica ($\%SiO_2 \cdot nH_2O$) assumed biogenic silica is 10% water by weight. Our precision for replicates of two sediment standards containing 12% and 30% biogenic silica was $\pm 4\%$ and $\pm 2\%$, respectively. There are no analytical determinations of a lithogenous portion of the sediment-trap samples. We have estimated the lithogenous flux by subtracting particulate organic matter (POM), biogenic silica and calcium carbonate from the total dry weight. POC is converted to POM by assuming an atomic ratio of organic carbon to phosphorus of 106/1 (Redfield *et al.*, 1963) and by using the ratio of nitrogen to organic carbon (N/C by atom) of each sample to create the model organic molecule $(CH_2O)_{106}(NH_3)_x(H_3 PO_4)$, where $x = 106$ N/C. For the range of N/C observed in Sechelt (0.12–0.066 by atom), multiplication of POC by 2.7 (range 2.67 to 2.74) provides an estimate of POM.

c. Estimating anticipated and additional fluxes

From the flux observations we had hoped to find decreases with depth and therefore be able to quantify organic carbon remineralization and water-column oxygen demand (Timothy, 1994). However, sediment-trap fluxes often increased with depth during the experiment. We attempt to find characteristic decay constants by partitioning the flux to a deeper trap into two components. The first is the observed flux to a shallow trap, corrected for decay between the traps. It is termed the *anticipated flux* because, having passed the depth of a shallow trap, we assume it will reach a deeper trap. The second component of flux is that material caught by a deeper trap in excess of the anticipated flux, referred to as the *additional flux*. Thus, the observed flux to a deeper trap is the sum of anticipated and additional fluxes, while the flux to shallow traps is not separable into these components. The anticipated flux might be related to the primary flux settling through the water column for the first time, but we do not use the term *primary* in our modeling because it is possible that the flux to an upper trap is influenced by processes such as secondary settling material and imperfect trapping efficiency so that the observed flux at shallow traps might be different than the true primary flux. Figure 2 is a schematic presentation of anticipated and additional fluxes.

Fluxes are recorded by two sediment traps at depths z_1 and z_2 (z is positive downward). We denote j as a component of the total dry-weight flux, J. Anticipated and additional fluxes are identified by subscripts n and d, respectively, k_j (m^{-1}) is a depth decay constant for component j, and $(j/J)_d$ is the fraction of component j in the total additional flux.
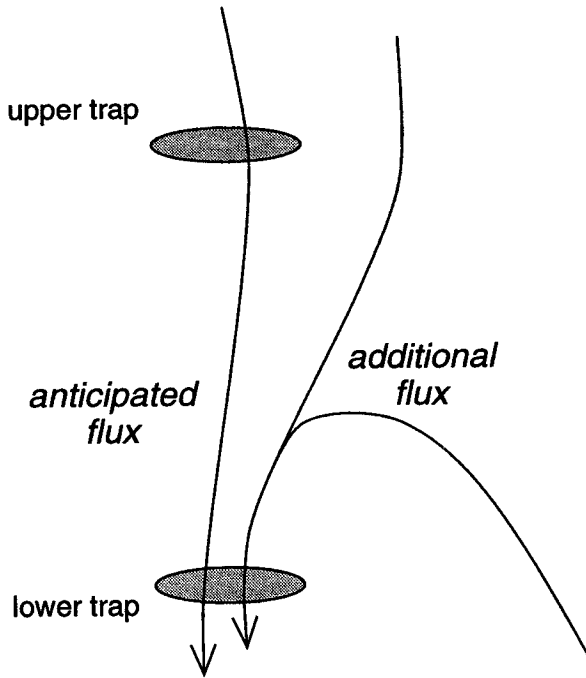
Figure 2. Schematic diagram of anticipated and additional fluxes. Additional fluxes may originate in surface and/or subsurface regions.

Assuming that the amount of decay of component j is a constant proportion of the flux of j, the anticipated flux of component j at z_2 is written as $j_n = j_1\, e^{-k_j \Delta z}$ where Δz is $z_2 - z_1$. Therefore, the total flux of component j at z_2 can be written as $j_2 = j_1\, e^{-k_j \Delta z} + j_d$. We wish to find k_j, but j_d is also unknown and is likely to be unpredictable. However, $(j/J)_d$ may be better constrained than j_d. We use the identity $j_d = (j/J)_d J_d$ to write:

$$ j_2 = j_1\, e^{-k_j \Delta z} + \left(\frac{j}{J}\right)_d J_d. \tag{1} $$

Eq. 1 is a linear equation with the form $y = ax_1 + bx_2 + constant$. The variables are j_2, j_1 and J_d, while the parameters that we wish to find are $e^{-k_j \Delta z}$ and $(j/J)_d$. The constant is implied to be zero in Eq. 1. An expression for the variable J_d is discussed next.

If fluxes do not decay as they pass from upper to lower traps, the additional flux will be the difference in observed flux between the two traps, $J_2 - J_1$. If water-column decay does occur, J_d will be greater than $J_2 - J_1$ by the amount of J_1 that is lost. Lithogenous fluxes are expected to be conservative (later verified) and $CaCO_3$ made up only about 1% of observed fluxes in Sechelt Inlet. If the degradation of POM and POC are similar, then

$$ J_d = J_2 - J_1 + 2.7\, C_1(1 - e^{-k_C \Delta z}) + Si_1(1 - e^{-k_{Si} \Delta z}). \tag{2} $$

C_1 and Si_1 are fluxes of organic carbon and biogenic silica at the depth of an upper sediment trap, k_C and k_{Si} are decay constants for organic carbon and biogenic silica, and the factor 2.7 is used to convert POC to POM. In Eq. 2, the terms with C_1 and Si_1 account for the part of J_1 lost to the water column between depths z_1 and z_2. Replacing J_d of Eq. 1 with Eq. 2,

$$j_2 = j_1\, e^{-k_j \Delta z} + \left(\frac{j}{J}\right)_d (J_2 - J_1 + 2.7C_1\{1 - e^{-kc\Delta z}\} + Si_1\{1 - e^{-ksi\Delta z}\}). \tag{3}$$

If one has estimates of k_C and k_{Si} (explained below), the variables of Eq. 3 are known for a single sediment-trap deployment and depth interval. Given n deployments at a particular depth interval, a set of n equations with three unknowns (the two parameters and the constant as described for Eq. 1) can be constructed and the unknowns can be solved in a least-squares sense using multivariate linear regression. If the processes controlling observed fluxes for a particular depth interval are consistent over many deployments, then the decay rate of anticipated fluxes and the composition of additional fluxes may be well constrained and Eq. 3 should be a good descriptor of those sediment-trap records. But, if k_j and $(j/J)_d$ are extremely variable over a multi-deployment period, then the model will not fit well to observed fluxes. Note that constancy of k_j and $(j/J)_d$ throughout a multi-deployment experiment can occur whether or not there is variability in the *amounts* of anticipated and additional material delivered to a deeper trap, and whatever the cause of additional fluxes.

3. Results

a. Comparison of sample treatments

Paried *t*-tests were conducted on fluxes to traps with and without NaN_3; fluxes of total dry weight, organic carbon, nitrogen and biogenic silica were not significantly different. Therefore, all reported data are averages of the two treatments at each depth and analyses are performed on these averages. Figures 3, 4 and 5 present total and constituent fluxes at each station and depth. C/N by weight is given instead of nitrogen fluxes. Percentages of the total flux for organic carbon, biogenic silica and lithogenous matter are also reported.

Consistent with the buffering effect of NaN_3 on the dissolution of $CaCO_3$ (Knauer and Asper, 1989), observed fluxes of $CaCO_3$ to the NaN_3-treated traps were greater than to the traps without NaN_3. We do not report $CaCO_3$ fluxes because they were only about 1% of the total during the experiment.

b. Temporal and spatial trends

Chlorophyll *a* concentrations and dominant phytoplankton throughout the study are shown in Figure 6. The February deployment occurred prior to the onset of the spring bloom, which began sometime during the March deployment and likely continued into the April sampling period. During the May and June deployments, the phytoplankton passed through a transition from diatom to flagellate predominance. Evidence for grazers in
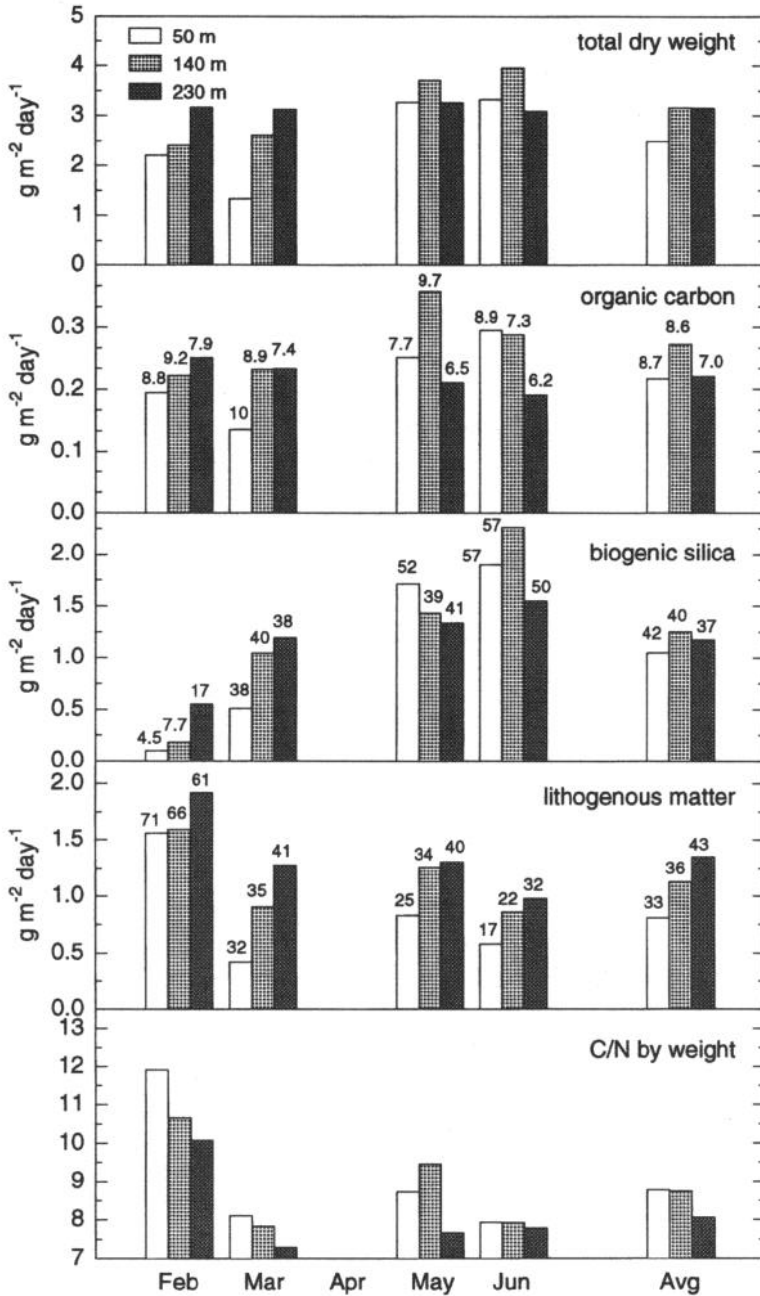
Figure 3. Observed fluxes and C/N at station SC-3. Numerical values at the tops of the bars are percent of the total flux. Avg is the flux-weighted time average for the experiment. In April, the mooring was lost.
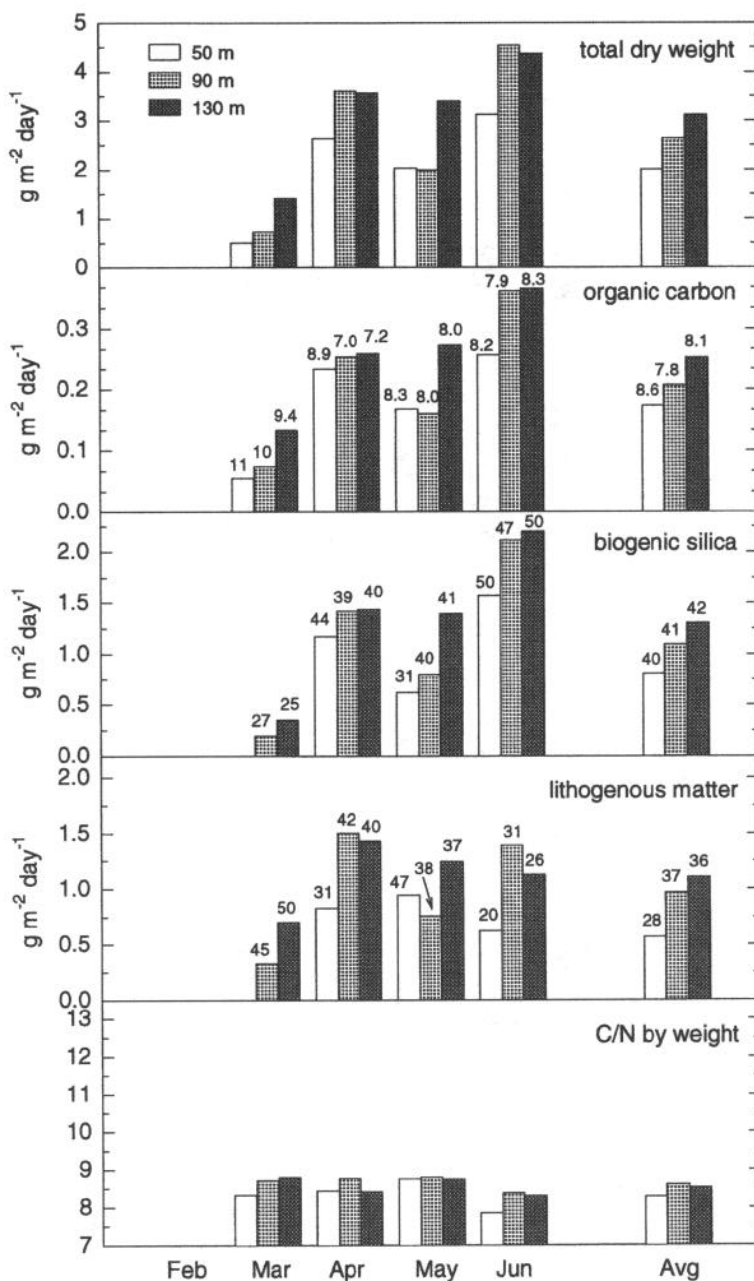
Figure 4. Observed fluxes and C/N at station SC-5.5. Numerical values at the tops of the bars are percent of the total flux. Avg is the flux-weighted time average for the experiment. The first deployment was in March when not enough sample was collected in the upper traps for analysis of biogenic silica.
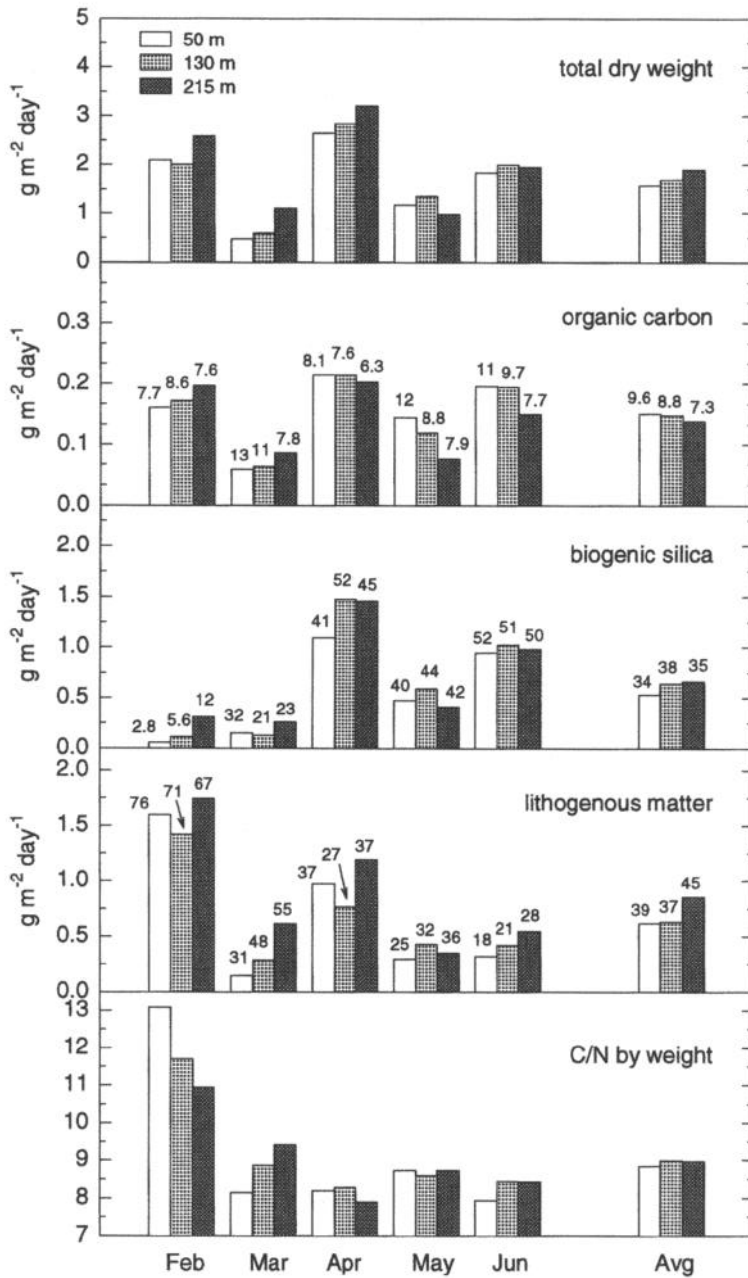
Figure 5. Observed fluxes and C/N at station SC-7. Numerical values at the tops of the bars are percent of the total flux. Avg is the flux-weighted time average for the experiment.
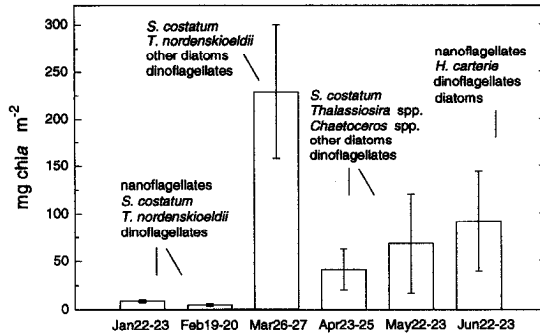
Figure 6. Chlorophyll *a* vertically integrated to 1% surface irradiance and averaged over five stations throughout Sechelt Inlet. The error bar is ± one standard deviation. Dominant phytoplankton are reported in decreasing abundance within each group. *S.* = *Skeletonema, T.* = *Thalassiosira, H.* = *Heterosigma*. Nanoflagellates were predominantly cryptomonads and *Chrysochromulina* spp.

surface waters at the ends of April, May and June included copepod nauplii, planktonic larvae, large populations of ciliates and heterotrophic dinoflagellates. In general, phytoplankton species composition and abundance closely resembled that for the previous two to three years (Haigh *et al.,* 1992).

Figures 3, 4 and 5 show that total fluxes tended to increase seaward, being lowest at station SC-7, intermediate at SC-5.5 and highest at SC-3. Averaged over all deployment periods and depths, the fluxes at the three stations were 1.8, 2.7 and 3.0 g m^{-2} day^{-1}, respectively. Throughout the inlet for a given deployment period, there was only small variability in the composition of the observed flux. In February, compositions reflected refractory organic matter associated with wintertime fluxes. C/N was 10–13 and the lithogenous content was 61–76%, while biogenic silica was 2.8–4.5% in surface traps and increased to 12–17% in deep traps. The increase in biogenic silica with depth corresponded with a decrease in C/N and was possibly the result of sediment resuspended from the bottom and side-walls. Bottom sediments, an integration of the year's accumulation, could have been lower in C/N and higher in biogenic silica than winter primary fluxes. Beginning with the onset of the spring bloom and continuing throughout the experiment, C/N was 7.3–9.5, the lithogenous content was 17–55% and biogenic silica was 21–57%. Percent organic carbon did not show the degree of change of other constituents before and after the spring bloom. At all stations, organic carbon peaked in March reaching 10–13% in 50 m traps, and at station SC-7 it surpassed 10% in May and June. Otherwise, the organic carbon content was 6.2–9.7% at all stations, depths and deployments. The low organic carbon content of the sediment-trap fluxes may have been the result of dilution by diatomaceous silica and lithogenous matter.

In March and April, temporal variability in observed fluxes correlates with changes in the standing-stock of overlaying phytoplankton. During the accumulation of phytoplankton biomass in the euphotic zone in March, export fluxes were minimal, while the decline

in phytoplankton after March 26–27 coincided with a 3–4 fold increase in observed flux from the March to the April deployments at stations SC-5.5 and SC-7. In February, May and June, temporal changes in flux do not correlate with either phytoplankton biomass or changes in biomass. Poor temporal resolution of plankton abundance or a shift in the dynamics controlling export flux may have contributed to this lack of coherence. Also, terrestrial inputs of sinking material could have obscured the signal of autochthonous fluxes.

Decreases in the total flux with depth were observed during some deployments, for example in May and June between middle and lower traps at stations SC-3 and SC-7. But, averaged over the entire experiment, total fluxes at each station either increased or remained constant with depth (Figs. 3, 4 and 5). Fluxes of organic carbon tended to follow those of the total flux at the shallow station SC-5.5, but at SC-3 and SC-7 they were more likely to decrease with depth. Percent organic carbon most often decreased with depth while, except in February, C/N was irregular. Lithogenous fluxes always increased with depth at station SC-3 and usually at stations SC-5.5 and SC-7, while fluxes of biogenic silica always increased with depth at SC-5.5 and were variable at the other stations. There was little trend in changes with depth of percent biogenic silica while percent lithogenous matter usually increased with depth, except in February.

c. Application of the model to fluxes from Sechelt

One of the parameters of Eq. 3 is $e^{-k_j\Delta z}$. Therefore, application of Eq. 3 requires fluxes from a number of deployments but for the same depth interval to produce estimates of k_j. (Let D be the least-squares solution for $e^{-k_j\Delta z}$. Then, $k_j = -\ln(D)/\Delta z$.) For the data from Sechelt Inlet, there are only four or five records from sediment traps moored at given depth intervals. Such a small value for n does not provide satisfactory statistics when using multivariate linear regression to estimate the parameters of Eq. 3, so we would like to rearrange Eq. 3 in a way that fluxes from different depth intervals can be considered in the same analysis. That is, we would like to separate $-k_j$ from Δz in the exponent of the parameter $e^{-k_j\Delta z}$. To make this separation, the term $(-k_j j_1 \Delta z)$ is added to each side of Eq. 3 which is then rearranged.

$$j_2 - j_1(e^{-k_j\Delta z} + k_j\Delta z) = -k_j j_1 \Delta z$$
$$+ \left(\frac{j}{J}\right)_d (J_2 - J_1 + 2.7C_1\{1 - e^{-k_C\Delta z}\} + Si_1\{1 - e^{-k_{Si}\Delta z}\}). \quad (4)$$

In Eq. 4 the variables are $j_2 - j_1 (e^{-k_j\Delta z} + k_j\Delta z)$, $-j_1 \Delta z$ and $J_2 - J_1 + 2.7C_1 (1 - e^{-k_C\Delta z})$ $+ Si_1 (1 - e^{-k_{Si}\Delta z})$ and the parameters are k_j and $(j/J)_d$. Fitting Eq. 4 to data collected from different depth ranges and different stations compromises the results because depth- or station-dependent changes in the parameters $e^{-k_j\Delta z}$ (or k_j) and $(j/J)_d$ cannot be explored. Nonetheless, we will see that this treatment provides satisfactory estimates of the parameters k_j and $(j/J)_d$ for the sediment-trap fluxes from Sechelt Inlet.

The decay constants k_j, k_C and k_{Si}, are associated with variables of Eq. 4, so initially they

must be estimated to solve for the parameters k_j and $(j/J)_d$. We used zero as the first estimate of decay constants associated with variables, but retained the parameter k_j so that Eq. 4 reduced to:

$$j_2 - j_1 = -k_j j_1 \Delta z + \left(\frac{j}{J}\right)_d (J_2 - J_1).\qquad(5)$$

Second estimates of k_C and k_{Si} were made using multivariate linear regression (Wilkinson, 1989) to fit Eq. 5 to observed fluxes of organic carbon ($j = C$) and biogenic silica ($j = Si$). Putting the second estimates into the variables of Eq. 4 and using regression to fit Eq. 4 to fluxes of organic carbon and biogenic silica, improved estimates of k_C and k_{Si} were obtained. This iterative process on Eq. 4 was continued until the decay constants converged.

With the final estimates of k_C and k_{Si}, Eq. 4 was applied to fluxes of particulate nitrogen ($j = N$) and lithogenous matter ($j = L$). Decay constants for these components are not associated with the term for the additional flux, but iteration between the variable $j_2 - j_1$ ($e^{-k_j \Delta z} + k_j \Delta z$) and the parameter k_j was required. Again, we used zero as the first estimate for k_N and k_L. There is only one least-squares solution to Eq. 4 for a given set of data and the procedure always converged for the data from Sechelt Inlet. It is possible that the iterative procedure might not converge for some data sets, in which case a different first approximation for the decay constants would be needed.

In the previous section, we saw that the nature of fluxes changed from the February to the March deployments, but that from March to June the composition of observed fluxes was similar at all stations and depths. The compositional shift from low to high percent biogenic silica may have affected the composition of additional fluxes, and decay rates may have changed over this period. Therefore, we have fit Eq. 4 to the entire data set and to the subset collected from March through June. Values of k_j and $(j/J)_d$ are presented in Table 1. All model solutions were significant at $\alpha = 0.001$ and the fit to fluxes of organic carbon, nitrogen and biogenic silica was good ($r^2 = 0.82 - 0.91$). For lithogenous fluxes, $r^2 \approx 0.7$. The lower r^2 is not surprising, considering the indirect method by which the lithogenous content was estimated. Eq. 4 has the form $y = ax_1 + bx_2 + constant$ and, as mentioned earlier, the constant is implied to be zero. We did not constrain the constant during the fitting procedure and it was never statistically different from zero ($P \geq 0.19$ for the solution of constants when Eq. 4 was fit to C, Si, N and L). Solutions for the time intervals February–June and March–June were similar, indicating that the six data from February did not have a large influence on the results. The composition of the additional flux was nearly identical for the two model periods, while k for organic carbon, nitrogen and biogenic silica was somewhat larger for the March–June period.

We applied Eq. 4 to the lithogenous flux as a bench-mark for the model; no decay is expected, yet a lithogenous component of the additional flux should be detectable. The fit to Eq. 4 predicts that on average 39% of the additional flux was lithogenous, while there is no certainty that k_L was different from zero ($P > 0.05$). Another test of the solutions is that

Table 1. Results of fitting Eq. 4 to fluxes from Sechelt Inlet. Solutions for k_j and $(j/J)_d$ are given with their standard errors. P, the probability of falsely rejecting the null hypotheses H_0: $k_j = 0$ and H_0: $(j/J)_d = 0$, was less than 0.001 in all cases except for the decay of the lithogenous flux. n is the number of equations used for each fit, equivalent to the number of flux records from shallow-to-middle, shallow-to-deep and middle-to-deep sediment-trap depth intervals at all three stations.

	$k_j \ (10^{-3} \ \mathrm{m}^{-1})$	$\left(\dfrac{j}{J}\right)_d$ (%)	n	r^2
FEB–JUN				
C	4.6 ± 0.43	8.1 ± 0.85	39	0.83
N	4.2 ± 0.35	0.97 ± 0.085	39	0.86
Si	2.6 ± 0.31	42 ± 4.2	37	0.82
L	0.64 ± 0.41†	39 ± 4.3	37	0.71
MAR–JUN				
C	6.2 ± 0.41	8.5 ± 0.81	33	0.91
N	4.8 ± 0.34	1.0 ± 0.083	33	0.90
Si	3.3 ± 0.36	42 ± 4.7	31	0.83
L	1.5 ± 0.82††	39 ± 4.9	31	0.70

†$P = 0.12$
‡$P = 0.083$

the contents of the components of the additional flux should add to 100% of the additional flux. From Table 1 and letting 2.7 $(C/J)_d$ be an estimate of $(POM/J)_d$, the sum of the organic, siliceous and lithogenous components of the additional flux was 103% for Feb–Jun and 104% for Mar–Jun. These values would be higher by about 1% if additional fluxes of $CaCO_3$ were considered.

To illustrate the solutions to Eq. 4, the variables can be plotted in three-dimensional space and the plane representing the least-squares fit can be superimposed onto the plot. In such a figure, the slopes of the lines representing the intersections of the plane with the $y:x_1$ and $y:x_2$ surfaces (where y, x_1 and x_2 are the variables of Eq. 4) are the best estimates of parameters k_j and $(j/J)_d$. Visualizing these slopes and the positioning of data points relative to the solution plane on the two-dimensional page is not straightforward. Therefore, to illustrate the solution for organic carbon (Fig. 7), we have divided Eq. 4 by $C_1 \Delta z$ to create a two-dimensional relationship where the slope of plotted data is $(C/J)_d$ and the y-intercept is $-k_C$. This treatment will result in a greater correlation between the new variables if $r^2 < 1$ of the original three-dimensional model. In fact, r^2 of the least-squares fit to Figure 7 (not shown) is 0.91, while $r^2 = 0.83$ for the equivalent three-dimensional solution (Table 1). Two-dimensional plots for N, Si and L are similar to that for C, but the slopes, y-intercepts and correlations reflect the estimates of k_j and $(j/J)_d$ and the r^2 values of Table 1.

From the fits of Eq. 4 to these sediment-trap fluxes (Table 1), there appears to have been a degree of spatial and temporal constancy in k_j and $(j/J)_d$ during the experiment in Sechelt Inlet, justifying the use of the model. The February–June decay constants predict that, for a 200 m depth interval, $60 \pm 3\%$ of the POC flux, $57 \pm 3\%$ of the nitrogen flux, and $41 \pm 4\%$ of sinking biogenic silica were lost from the particulate phase.
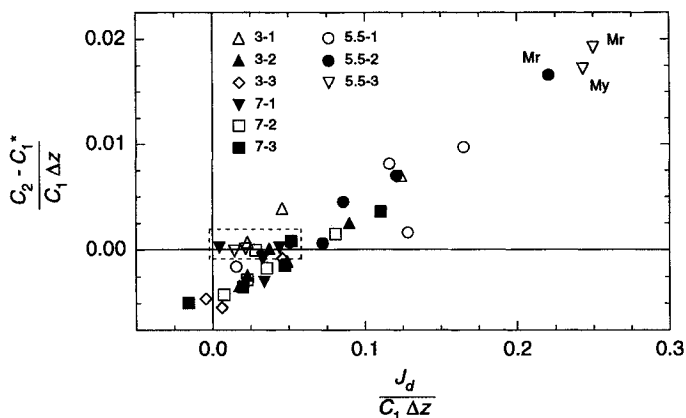
Figure 7. Two-dimensional illustration of the model applied to sediment-trap fluxes of organic carbon. The plot is created by dividing Eq. 4 by $C_1\Delta z$ so that the slope of the plot is $(C/J)_d$ and the y-intercept is $-k_C$. $C_1^* = C_1 (e^{-k_C\Delta z} + k_C\Delta z)$ and $J_d = (J_2 - J_1 + 2.7C_1\{1 - e^{-k_C\Delta z}\} + Si_1\{1 - e^{-k_{Si}\Delta z}\})$. The February data are six of the points within the dashed box. The month of collection for three of the points is noted: Mr = March, My = May. Different symbols represent different sediment-trap depth intervals; 3, 5.5 and 7 are stations and 1, 2 and 3 are shallow-to-middle, shallow-to-deep and middle-to-deep depth intervals, respectively.

4. Discussion

a. Particulate decay

The results of flux decay (Table 1) are self-consistent in that the decay of carbon and nitrogen were similar, the decay of biogenic silica was somewhat lower and there was no significant decay of the lithogenous flux. For comparison, Wassmann (1983) estimated that about 75% of the POC supply to deeper stagnant waters in Lindåsopollene was lost to heterotrophic respiration and advective export from the fjord. This loss is very large, as it occurred over a depth interval of only 20 m. In Nordåsvannet, fluxes of POC decreased by about 30% over a 45 m depth interval, but the traps may have missed the sharpest decrease in POC flux because they were farther from the base of the euphotic zone than the traps in Lindåspollene (Wassmann, 1985). In Sechelt, the top traps were 30 m or more from the base of the euphotic zone, farther than in both of Wassmann's studies. Bishop (1989) summarized eight regression equations of POC flux in oceanic settings. Most of those relationships include terms for primary production, but predictions of depth-dependent changes in flux can be made by holding primary production constant. Ocean fluxes decrease most rapidly near the surface. For the uppermost 200 m relevant to each (either 50–250 m or 100–300 m), the oceanic relationships predict that POC flux decreases by between 50 and 77%. Our results give a 60% loss of the POC flux over a 200 m depth change, or 71% using the value of k_C from the March–June data.

Interestingly, although the decay rates for organic carbon and nitrogen were similar for the February–June period, the decay rate of organic carbon was greater than that for

Table 2. Rates of biogenic silica dissolution (V_{dis}) converted to the sinking rate equivalent required for the average k_{Si} of Table 1 (0.003 m^{-1}). *S. costatum* and *T. nordenskioeldii* were the predominant diatoms during most of the study in Sechelt; *R. hebetata* has a strongly siliceous frustule and thus low V_{dis}. V_{dis} for *S. costatum* from Paasche and Østergreen (1980), for *T. decipiens* and *R. hebetata* from Kamatani and Riley (1979), for *T. pseudonana* from Nelson et al. (1976), and for the field experiment from Nelson and Goering (1977). *S.* = *Skeletonema*, *T.* = *Thalassiosira*, *R.* = *Rhizosolenia*, n.a. = not available.

Species	Temp °C	Laboratory or field	V_{dis} (10^{-3} hr^{-1})	sr equiv (m day^{-1})
S. costatum†	20	lab	9.5	76
T. decipiens	11	lab	2.5–39	20–310
R. hebetata	11	lab	1.1–5.1	8.8–41
T. pseudonana				
coastal	20	lab	7.5–8.5	60–68
oceanic	20	lab	2.0–4.3	16–34
n.a.	n.a.	field	3.8–23‡	30–180

†Unpubl. results: 0.016 pg Si cell^{-1} hr^{-1} dissolved for avg. Si cell^{-1} of 1.7 pg. We use $V_{dis} = -\ln (Si_t/Si_{t_0})/\Delta t$.

‡Range for 7 vertically averaged profiles; mean = 0.01 hr^{-1} with *sr equiv* of 180 m day^{-1}.

nitrogen from March to June. This result contradicts the general observation that nitrogen tends to degrade from organic material faster than carbon (e.g. Toth and Lerman, 1977), but Harvey et al. (1995) observed that phytoplankton carbohydrates were lost more rapidly than proteins or lipids under oxic conditions during laboratory experiments of organic decay. Perhaps nitrogen-deplete carbohydrates were a large part of the decaying organic flux from March until June.

To evaluate our estimates of biogenic silica decay, we compare them to time-dependent dissolution of diatomaceous silica (V_{dis}: time^{-1}). The sinking rate equivalent required to translate k_{Si} to V_{dis} can be calculated from: *sr equiv* = V_{dis}/k_{Si}. Because the rate of dissolution of biogenic silica varies among species of diatoms (Lewin, 1961; Kamatani, 1971), we emphasize the comparison for the dominant diatom during the study, *S. costatum*. The agreement of the sinking rate equivalents of Table 2 to sinking rates for marine aggregates and fecal pellets (likely vehicles for sinking biogenic silica) of the order 100 m day^{-1} (see Alldredge and Gotschalk, 1988; Fowler and Knauer, 1986; and references in both for similarities and exceptions) suggests that our results for k_{Si} are consistent with values reported for V_{dis}.

b. Additional fluxes

i. Quantification and bulk composition. Using Eq. 2 and noting that $J_n = J_2 - J_d$, we separated the measured fluxes to deeper traps into their anticipated and additional components (Fig. 8). Although there were sometimes decreases in observed flux with depth (Figs. 3, 4 and 5), only once were measured fluxes less than anticipated (SC-7 in May to the deepest trap). Thus, the vertical pattern of flux during the experiment must have been
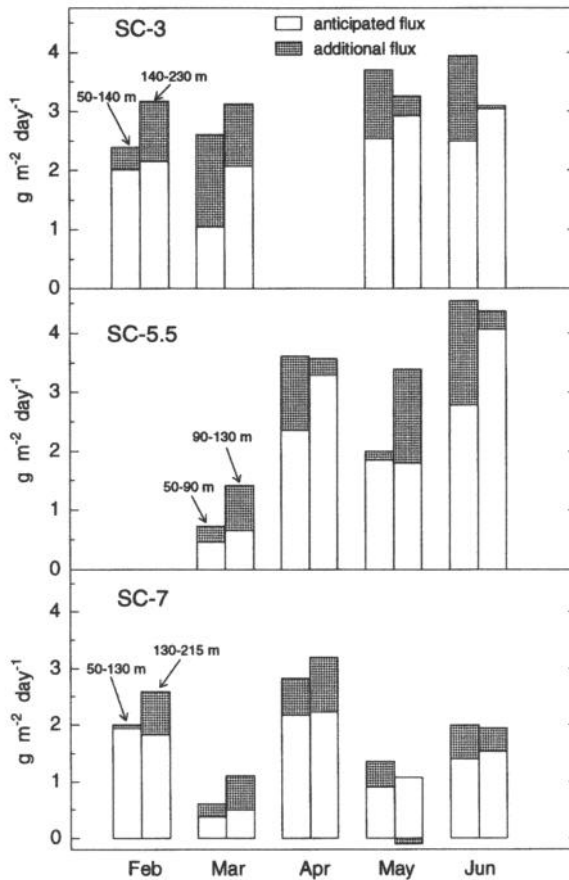
Figure 8. Anticipated and additional fluxes. Paired bars are for the shallow-to-middle and middle-to-deep sediment-trap depth intervals.

affected by the competing processes of water-column decay and the apparent addition of material with an unknown source to deeper traps.

Table 3 compares the mean composition of the anticipated flux, the additional flux and surficial bottom sediments collected by box core August 4–5, 1981. The composition of the anticipated flux to deeper traps was estimated for each deployment in two ways: first by the relationship $(j/J)_n = (j_1 e^{-k_j \Delta z})/J_n$, and second from $(j/J)_n = (j_2 - j_d)/J_n$. All variables on the right-hand side of each relationship were either measured directly or can be estimated from the results of Table 1, and the two methods gave similar results which were averaged for Table 3. The compositions of the anticipated and additional fluxes were very similar, although the additional flux may have been slightly enriched in biogenic silica for the February–June deployments and in organic carbon from March until June. Surficial sediments from a decade earlier were depleted in biogenous and higher in lithogenous

Table 3. Mean composition of anticipated and additional fluxes, and of surficial bottom sediments taken from core tops collected August 4–5, 1981. The composition of the anticipated flux is estimated from two methods described in the text and of the additional flux is taken from Table 1. C/N is by weight. No core was taken at station SC-5.5. The composition at SC-5.5 is determined as the mean of a core three km up-inlet and another three km down-inlet of SC-5.5.

	Anticipated fluxes†		Additional fluxes‡		Surficial bottom sediment		
	Feb–June	Mar–Jun	Feb–Jun	Mar–Jun	SC-3	SC-5.5	SC-7
%C	7.2	7.2	8.1	8.5	6.1	6.2	6.5
%N	0.87	0.92	0.97	1.0	0.60	0.61	0.65
%Si	33	38	42	42	34	28	44
%L	45	39	39	39	50	55	38
C/N	8.3	7.8	8.4	8.5	10	10	10

†Fractional standard error less than the fractional standard error of the additional flux.
‡Standard error given in Table 1.

matter relative to additional fluxes to deep traps. C/N of bottom sediments was also higher than C/N of the additional flux.

Resuspended bottom sediment is often intercepted during sediment-trap experiments and typically causes observed fluxes to increase most dramatically as the bottom is approached (e.g. Dymond, 1984; Hedges *et al.,* 1988a; Gardner and Richardson, 1992; Overnell and Young, 1995; Pejrup *et al.,* 1996). In contrast, Wassmann (1983; 1985) found that resuspension was minimal for two 90 m deep land-locked fjords and sediment-trap flux substantially decreased with depth. Because of friction between tidal currents and topography at Skookumchuck Narrows, tidal energy is minimal in Sechelt Inlet. Estuarine circulation is not strong as freshwater input is small, and the north–south situation of the inlet protects it from local winds that generally blow southeast–northwest. These features make Sechelt a characteristically low energy inlet, and may explain why additional fluxes were sometimes small (Fig. 8). Resuspended material reflecting the composition of bottom sediments may have reached deeper traps in February and sporadically at other times during the study. However, the relative composition of additional fluxes (Table 3) and the pattern of flux change with depth (increases often being most pronounced to mid-depths) suggest that bulk sediment resuspension was not the only cause of additional fluxes.

ii. Other possible causes of additional fluxes. As they descend in a narrowing inlet, particles might mix inward and their concentration increase. Particle focusing toward the center of an inlet is maximized if material does not become associated with the sides as it sinks, and lateral eddy diffusion is large enough to remove lateral gradients in particle density. The maximum degree of particle focusing is W_1/W_2, where W_1 and W_2 are the widths of the inlet at depths z_1 and z_2. Averaged for the entire experiment, changes in flux with depth were similar to W_1/W_2 at SC-5.5 and less at stations SC-3 and SC-7. For this reason, and because the composition of inwardly focused material is not likely to have

differed substantially from material sinking through the center of the inlet, particle focusing may have contributed additional fluxes to deeper traps.

Other mechanisms by which compositionally "fresh" material may be added to deeper traps include hydrodynamic sorting of biogenous from heavier lithogenous resuspended sediment (Smetacek, 1980) and the rebound of primary settling aggregates off the sides and floor of the inlet (Walsh *et al.*, 1988b; Walsh and Gardner, 1992). If occurring most intensely along side-walls at shallow to mid-depths in Sechelt Inlet, either process could have caused pronounced additional fluxes to the mid-depth sediment traps. In fact, inward focusing (discussed above), rebound flux and hydrodynamic sorting are related mechanisms, acting on different time scales, by which compositionally similar particles may move from the sides toward the center of the inlet. Our use of sediment traps alone cannot discern which of these processes, if any, dominantly contributed to additional fluxes.

Horizontal advection is a means by which surface-leaving fluxes may be transported away from the region of their origin. Indeed, particles can travel a long distance before reaching sediment traps at depth (e.g. Deuser *et al.*, 1988). If, while they are sinking, advection moves particles from areas of high export flux to regions where export is low, sediment traps moored in the low-export waters may record increases in flux with depth. We performed a scale analysis to test whether vertical changes in flux might have been caused by horizontal gradients in the export flux (H: g m^{-2} day^{-1} m^{-1}) and horizontal advection (u: cm s^{-1}). Our analysis tests the relationship: $dJ/dz = Husr^{-1}$, where sr is sinking rate. Observed fluxes at 50 m suggest that during the experiment the export flux increased seaward, and there was a net inflow velocity of about 1 cm s^{-1} and less at 100 m at station SC-3 (Tinis, 1995). Making an estimate of H from observed fluxes, horizontal advection could have accounted for a substantial fraction of the additional fluxes only if sinking rates were less than about 20 m day^{-1}.

Material that was grazed near the surface and defecated at depth by dielly migrating zooplankton contributed less than 1% of the pigment flux during a study in Dabob Bay, WA (Dagg *et al.*, 1989). Because the dielly migrating copepods *Calanus pacificus* and *Metridia lucens* are common to both Dabob Bay and Sechelt Inlet (Dagg *et al.*, 1989; R. Goldblatt unpubl.), we consider active transport by zooplankton to have been an unlikely cause of the additional fluxes.

iii. Trapping efficiency. Dimensional analysis has shown that for a cylindrical trap with a given aspect ratio, trapping efficiency is proportional to sr and to the inverse of sediment trap Reynolds number Re (Butman *et al.*, 1986). Smetacek *et al.* (1978) attributed observed increases in flux with depth in the Bornholm Basin to decreasing current speeds and increasing sinking rates with depth, leading to improved trapping efficiency for deeper sediment traps. Wassmann (1985) suggested that increases in the fluxes of chlorophyll *a* and particulate phosphorus at mid-depths in Nordåsvannet resulted from changes in trapping efficiency and mineralization within traps. Flume experiments found that trapping efficiency of cylindrical traps with aspect ratio of 3 decreased by a factor of two as Re

increased from 2,000 to 5,000, but then remained unchanged for Re up to 20,000 (Butman, 1986). For similar traps, internal turbulence occasionally reached the base of the collectors at $Re = 3,500$ and the bottom tranquil layer no longer existed at $Re = 6,000$ (Hawley, 1988), lending support to the results of Butman (1986). A field experiment by Baker *et al.* (1988) found that as Re surpassed 24,000, trapping efficiency decreased. However, they did not use cylindrical sediment traps, nor was their experiment sensitive to changes in trapping efficiency for $Re < 24,000$ (Baker *et al.*, 1988). Our sediment traps had an effective aspect ratio of 3.3 and they were baffled at the mouth. The baffles complicate comparison to the results of Butman (1986) and Hawley (1988), but Butman (1986) noted that the trapping efficiency of baffled and unbaffled traps was similar, while the variability for baffled traps was greater.

At station SC-3, the mean Reynolds number decreased from 5,500 at 50 m to 2,900 at 140 m, within the range where Butman (1986) found a two-fold decrease in trapping efficiency, and was similar at 140 and 230 m (Fig. 9). Vertical changes in Re leading to changes in trapping efficiency are consistent with the observation that fluxes often changed most dramatically between shallow and mid-depth traps, and similarity in composition between additional and anticipated fluxes may be expected if changes in trapping efficiency was a cause of additional flux. Thus, we cannot exclude the possibility that improved trapping efficiency with depth resulted in additional fluxes to deeper traps. That particles sinking faster in deeper waters may have further improved the collection efficiency of mid- and deep-water traps (Smetacek, 1978) might also be considered.

From this discussion we conclude that, as well as resuspension of sediment off the sides and bottom of the inlet, inward focusing of aggregates and improved trapping efficiency with depth were possible causes of additional fluxes during the study. Mid-depth, up-inlet advection of particle-rich waters was a less likely cause. The model we have used to interpret sediment-trap fluxes relies on operationally-defined terms (anticipated and additional fluxes) and the results (Table 1) are not affected by the mechanism of material addition to deeper traps; the anticipated flux had a characteristic rate of decay and the additional flux exhibited a mean composition. However, we have not extrapolated from operational fluxes to the true (primary plus resuspended) downward flux during the experiment. Such an extrapolation requires, in the least, better understanding of the causes of additional fluxes to deeper traps during the experiment. If the causes were mainly topographic focusing, resuspension and/or horizontal advection, then observed fluxes at all depths would be good estimates of true fluxes. But, if increasing trapping efficiency with depth were a cause of additional fluxes, then the best estimate of the true flux at any depth would be the observed flux to the deepest traps.

5. Summary

We have developed a model that allows estimates of the decay constants for constituents of sediment-trap fluxes when increased with depth are recorded. The model relies on an estimate of the composition of the additional flux, which is made simultaneously with
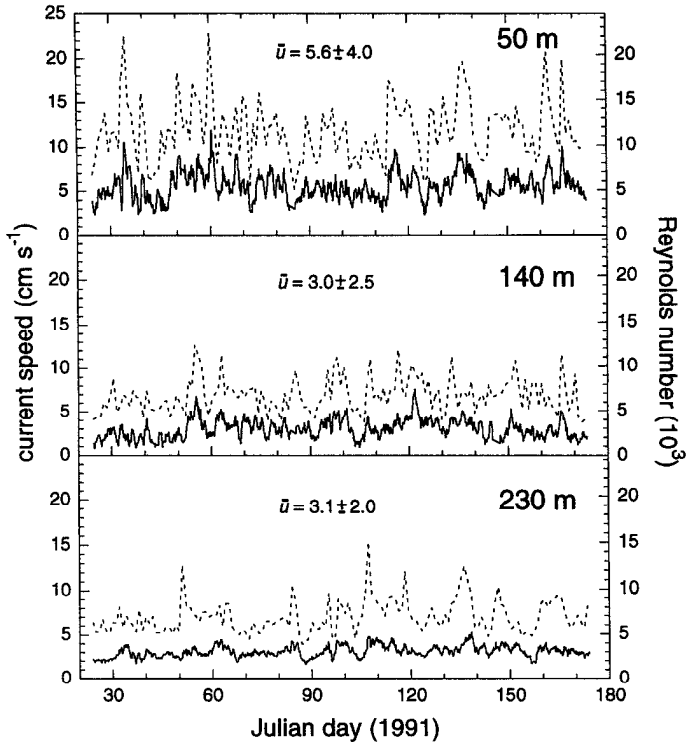
Figure 9. Current speed u at station SC-3 at sediment-trap depths. 24 hour running mean (solid line) and maximum speed for a 24 hour period (dotted line) are plotted. The mean current speed for the entire record at each depth is included $\pm$ its standard deviation. The right ordinate gives sediment-trap Reynolds number. $Re = uDv^{-1}$ where D is the inside trap diameter and v is kinematic viscosity. We have used $v = 0.013$ cm^2 s^{-1} for seawater of $T = 10°C$ and $S = 30$ so for our traps with D of 12.7 cm, $Re = 980u$.

decay constants. The results of fits to flux observations from Sechelt Inlet are self-consistent in that the decay of organic carbon and nitrogen were similar, the decay of biogenic silica was somewhat lower and there was no significant decay of the lithogenous flux. The results are also consistent with other estimates of organic carbon flux decay and with rates of dissolution of diatomaceous silica. The model we have used may be applied to other sediment-trap data sets, provided that decay constants and the composition of additional material change little. Given a larger body of data than that provided by the study in Sechelt, variations in decay constants with time and depth could be explored.

   Increases in sediment-trap flux with depth were often larger from shallow to mid-depth traps than from mid-depth to deep traps, and the composition of the additional flux was more similar to the composition of the anticipated flux than to the composition of bottom sediments sampled a decade earlier. However, we are unable to determine without ambiguity the cause of the additional fluxes. Sporadically and especially in February,

resuspended material may have reached deeper traps. Other factors that may have resulted in additional fluxes throughout the study include lateral particle mixing in the narrowing inlet and improved trapping efficiency in deeper waters.

REFERENCES

Alldredge, A. L. and C. Gotschalk. 1988. *In situ* settling behavior of marine snow. Limnol. Oceanogr., *33*, 339–351.

Baker, E. T., H. B. Milburn and D. A. Tennant. 1988. Field assessment of sediment trap efficiency under varying flow conditions. J. Mar. Res., *46*, 573–592.

Bishop, J. K. B. 1989. Regional extremes in particulate matter composition and flux: Effects on the chemistry of the ocean interior, *in* Productivity of the Oceans: Present and Past, W. H. Berger, V. S. Smetacek and G. Wefer, eds., Wiley, 117–137.

Bloesch, J. 1982. Inshore-offshore sedimentation differences resulting from resuspension in the Eastern Basin of Lake Erie. Can. J. Fish. Aquat. Sci., *39*, 748–759.

Butman, C. A. 1986. Sediment trap biases in turbulent flows: Results from a laboratory flume study. J. Mar. Res., *44*, 645–693.

Butman, C. A., W. D. Grant and K. D. Stolzenbach. 1986. Predictions of sediment trap biases in turbulent flows: A theoretical analysis based on observations from the literature. J. Mar. Res., *44*, 601–644.

Dagg, M. J., B. W. Frost and W. E. Walser, Jr. 1989. Copepod diel migration, feeding, and the vertical flux of pheopigments. Limnol. Oceanogr., *34*, 1062–1071.

Deuser, W. G., F. E. Muller-Kargen and C. Hemleben. 1988. Temporal variations of particle fluxes in the deep subtropical and tropical North Atlantic: Eulerian versus Lagrangian effects. J. Geophys. Res., *93*, 6857–6862.

Dymond, J. 1984. Sediment traps, particle fluxes, and benthic boundary layer processes, *in* Workshop on the Global Ocean Flux Study Proceedings, National Academy Press, 260–284.

Falkowski, P. G., P. E. Biscaye and C. Sancetta. 1994. The lateral flux of biogenic particles from the eastern North American continental margin to the North Atlantic Ocean. Deep-Sea Res. II, *41*, 583–601.

Fowler, S. W. and G. A. Knauer. 1986. Role of large particles in the transport of elements and organic compounds through the oceanic water column. Prog. Oceanogr., *16*, 147–194.

Gardner, W. D. 1980. Field assessment of sediment traps. J. Mar. Res., *38*, 41–52.

Gardner, W. D. and M. J. Richardson. 1992. Particle export and resuspension fluxes in the western North Atlantic, *in* Deep-Sea Food Chains and the Global Carbon Cycle, G. T. Rowe and V. Pariente, eds., Kluwer, 339–364.

Haigh, R., F. J. R. Taylor and T. F. Sutherland. 1992. Phytoplankton ecology of Sechelt Inlet, a fjord system on the British Columbia coast. I. General features of the nano- and microplankton. Mar. Ecol. Prog. Ser., *89*, 117–134.

Håkanson, L., S. Floderus and M. Wallin. 1989. Sediment trap assemblages—a methodological description. Hydrobiologia, *176/177*, 481–490.

Harvey, H. R., J. H. Tuttle and J. T. Bell. 1995. Kinetics of phytoplankton decay during simulated sedimentation: Changes in biochemical composition and microbial activity under oxic and anoxic conditions. Geochim. Cosmochim. Acta, *59*, 3367–3377.

Hasle, G. R. 1978. Using the inverted microscope, *in* Phytoplankton Manual. Monographs on Oceanographic Methodology *6*, A. Sornia, ed., UNESCO, 191–196.

Hawley, N. 1988. Flow in cylindrical sediment traps. J. Great Lakes Res., *14*, 76–88.

Hedges, J. I., W. A. Clark and G. L. Cowie. 1988a. Fluxes and reactivities of organic matter in a coastal marine bay. Limnol. Oceanogr., *33*, 1137–1152.

—— 1988b. Organic matter sources to the water column and surficial sediments of a marine bay. Limnol. Oceanogr., *33*, 1116–1136.

Kamatani, A. 1971. Physical and chemical characteristics of biogenous silica. Mar. Biol., *8*, 89–95.

Kamatani, A. and J. P. Riley. 1979. Rates of dissolution of diatom silica walls in seawater. Mar. Biol., *55*, 29–35.

Knauer, G. and V. Asper. 1989. Sediment trap technology and sampling. Report of the U.S. Global Ocean Flux Study Working Group on Sediment Trap Technology and Sampling, November 1988. U.S. GOFS planning report no. 10, August 1989, 94 pp.

Lewin, J. C. 1961. The dissolution of silica from diatom walls. Geochim. Cosmochim. Acta, *21*, 182–198.

Mortlock, R. A. and P. N. Froelich. 1989. A simple method for the rapid determination of biogenic opal in pelagic marine sediments. Deep-Sea Res., *36*, 1415–1426.

Nelson, D. M. and J. J. Goering. 1977. Near-surface silica dissolution in the upwelling region off northwest Africa. Deep-Sea Res., *24*, 65–73.

Nelson, D. M., J. J. Goering, S. S. Kilham and R. R. L. Guillard. 1976. Kinetics of silicic acid uptake and rates of silica dissolution in the marine diatom *Thalassiosira pseudonana.* J. Phycol., *12*, 246–252.

Noriki, S. and S. Tsunogai. 1986. Particulate fluxes and major components of settling particles from sediment trap experiments in the Pacific Ocean. Deep-Sea Res., *33*, 903–912.

Orians, K. J. and K. W. Bruland. 1986. The biogeochemistry of aluminum in the Pacific Ocean. Earth Planet. Sci. Lett., *78*, 397–410.

Overnell, J. and S. Young. 1995. Sedimentation and carbon fluxes in a Scottish sea loch, Loch Linnhe, Estuar. Coast. Shelf Sci., *41*, 361–376.

Paasche, E. and I. Østergren. 1980. The annual cycle of plankton diatom growth and silica production in the inner Oslofjord. Limnol. Oceanogr., *25*, 481–494.

Parsons, T., Y. Maita and C. Lalli. 1984. A Manual of Clinical and Biological Methods of Seawater Analysis, Pergamon, 173 pp.

Pejrup, M., J. Valeur and A. Jensen. 1996. Vertical fluxes of particulate matter in Aarhus Bight, Denmark. Cont. Shelf Res., *16*, 1047–1064.

Pickard, G. L. 1961. Oceanographic features of inlets in the British Columbia mainland coast. J. Fish. Res. Board Can., *18*, 907–999.

Redfield, A. C., B. H. Ketchum and F. A. Richards. 1963. The influence of organisms on the composition of sea-water, *in* The Sea, M. N. Hill, ed., Wiley, 26–77.

Smetacek, V. 1980. Annual cycle of sedimentation in relation to plankton ecology in western Kiel Bight. Ophelia (Suppl.), *1*, 65–76.

Smetacek, V., K. von Brockel, B. Zeitzschel and W. Zenk. 1978. Sedimentation of particulate matter during a phytoplankton spring bloom in relation to the hydrographical regime. Mar. Biol., *47*, 211–226.

Sutherland, T. F., C. Leonard and F. J. R. Taylor. 1992. A segmented pipe sampler for integrated profiling of the upper water column. J. Plank. Res., *14,* 915–923.

Timothy, D. A. 1994. Production and consumption of organic carbon and oxygen in Sechelt Inlet, British Columbia, M.Sc. thesis, University of British Columbia, 174 pp.

Tinis, S. 1995. The circulation and energetics of the Sechelt Inlet System, British Columbia, Ph.D. thesis, University of British Columbia, 173 pp.

Toth, D. J. and A. Lerman. 1977. Organic matter reactivity and sedimentation rates in the ocean. Am. Jour. Sci., *277,* 465–485.

Walsh, I., J. Dymond and R. Collier. 1988a. Rates of recycling of biogenic components of settling particles in the ocean derived from sediment trap experiments. Deep-Sea Res., *35,* 43–58.

Walsh, I., K. Fischer, D. Murray and J. Dymond. 1988b. Evidence for resuspension of rebound particles from near-bottom sediment traps. Deep-Sea Res., *35,* 59–70.

Walsh, I. D. and W. D. Gardner. 1992. A comparison of aggregate profiles with sediment trap fluxes. Deep-Sea Res., *39,* 1817–1834.

Wassmann, P. 1983. Sedimentation of organic and inorganic particulate material in Lindåspollene, a stratified, land-locked fjord in western Norway. Mar. Ecol. Prog. Ser., *13,* 237–248.

—— 1985. Sedimentation of particulate material in Nordåsvaninet, a hypertrophic, land-locked fjord in western Norway. Mar. Ecol. Prog. Ser., *22,* 259–271.

Wilkinson, L. 1989. SYSTAT: The System for Statistics, SYSTAT, Inc., Evanston, IL, 638 pp.